

Technical Note

# Enhancing Variant Prioritization in VarFish through On-Premise Computational Facial Analysis

Meghna Ahuja Bhasin <sup>1</sup>, Alexej Knaus <sup>1</sup>, Pietro Incardona <sup>1,2</sup>, Alexander Schmid <sup>1</sup>, Manuel Holtgrewe <sup>3</sup>, Miriam Elbracht <sup>4</sup>, Peter M. Krawitz <sup>1</sup> and Tzung-Chien Hsieh <sup>1,\*</sup>

- <sup>1</sup> Institute for Genomic Statistics and Bioinformatics, University Hospital Bonn, Rheinische Friedrich-Wilhelms-Universität Bonn, 53127 Bonn, Germany; meghna@uni-bonn.de (M.A.B.); knausa@uni-bonn.de (A.K.); incardon@uni-bonn.de (P.I.); schmida@uni-bonn.de (A.S.); pkrawitz@uni-bonn.de (P.M.K.)
- <sup>2</sup> Core Unit for Bioinformatics Data Analysis, Medical Faculty, University of Bonn, 53127 Bonn, Germany
- <sup>3</sup> CUBI—Core Unit Bioinformatics, Berlin Institute of Health, 10117 Berlin, Germany; manuel.holtgrewe@bih-charite.de
- <sup>4</sup> Institute for Human Genetics and Genomic Medicine, Medical Faculty, RWTH Aachen University, 52062 Aachen, Germany; mielbracht@ukaachen.de
- \* Correspondence: thsieh@uni-bonn.de

**Abstract:** Genomic variant prioritization is crucial for identifying disease-associated genetic variations. Integrating facial and clinical feature analyses into this process enhances performance. This study demonstrates the integration of facial analysis (GestaltMatcher) and Human Phenotype Ontology analysis (CADA) within VarFish, an open-source variant analysis framework. Challenges related to non-open-source components were addressed by providing an open-source version of GestaltMatcher, facilitating on-premise facial analysis to address data privacy concerns. Performance evaluation on 163 patients recruited from a German multi-center study of rare diseases showed PEDIA's superior accuracy in variant prioritization compared to individual scores. This study highlights the importance of further benchmarking and future integration of advanced facial analysis approaches aligned with ACMG guidelines to enhance variant classification.

**Keywords:** variant prioritization; facial imaging analysis; next-generation phenotyping; rare diseases; exome sequencing analysis



**Citation:** Bhasin, M.A.; Knaus, A.; Incardona, P.; Schmid, A.; Holtgrewe, M.; Elbracht, M.; Krawitz, P.M.; Hsieh, T.-C. Enhancing Variant Prioritization in VarFish through On-Premise Computational Facial Analysis. *Genes* **2024**, *15*, 370. <https://doi.org/10.3390/genes15030370>

Academic Editors: Martina Witsch-Baumgartner and Beatrix Mühlegger

Received: 6 February 2024  
Revised: 3 March 2024  
Accepted: 13 March 2024  
Published: 17 March 2024



**Copyright:** © 2024 by the authors. Licensee MDPI, Basel, Switzerland. This article is an open access article distributed under the terms and conditions of the Creative Commons Attribution (CC BY) license (<https://creativecommons.org/licenses/by/4.0/>).

## 1. Introduction

Approximately 6% of the worldwide population is affected by rare diseases [1]. Whole exome sequencing (WES) has been proven to facilitate the diagnosis of rare diseases [2]. However, analyzing the tremendous variants generated by WES has become an issue. Therefore, efficiently prioritizing the variants relies on algorithms, databases, and annotations to assess and rank variants based on many parameters, including the predicted impact on protein structure and function, population frequency, and associations with established diseases.

In addition to analyzing the properties of the variants, utilizing clinical phenotypes to help the diagnosis is crucial. As patients' clinical phenotypes can be documented by the Human Phenotype Ontology (HPO) terminology [3], many computational approaches have been developed based on HPO terms to diagnose rare diseases [4–16]. In addition, many rare diseases often present a characteristic pattern of facial features called “facial gestalt”. With the recent advances in computer vision, the next-generation phenotyping (NGP) approaches that analyze a patient's frontal image have proven capable of diagnosing patients with rare disorders [17–26]. The Prioritization of Exome Data by Image Analysis (PEDIA) study has demonstrated that integrating facial and clinical feature analysis into variant prioritization significantly improves performance [27]. However, the facial analysis

approach employed in the original PEDIA study, namely DeepGestalt [21], was facilitated by Face2Gene, a proprietary tool that poses challenges for seamless integration. In 2023, GestaltMatcher [25], the extension to DeepGestalt, released the open-source version [28] that trains on GestaltMatcher Database [29] compliant with the findability, accessibility, interoperability, and reusability (FAIR) principles. This update offered an on-premise solution for conducting facial analysis. Hence, the critical aspect lies in effectively facilitating the integration of these tools into the variant prioritization process.

This study showcased how we integrated facial analysis (GestaltMatcher) and feature analysis (CADA [12]) into VarFish [30], an open-source framework designed for variant analysis (Figure 1). VarFish provides a user-friendly interface and visualization tools that facilitate efficient exploration and interpretation of variants, enabling analysts to navigate complex genomic data easily. We further performed performance benchmarking on 163 patients enrolled in TRANSLATE-NAMSE (TNAMSE), a German national rare disorder project [26]. Each patient contained HPO terms, a facial image, and exome data. The integration of VarFish with GestaltMatcher exemplifies the capability to analyze any medical images within a variant analysis platform. It is essential for users seeking the on-premise solution because of privacy concerns.

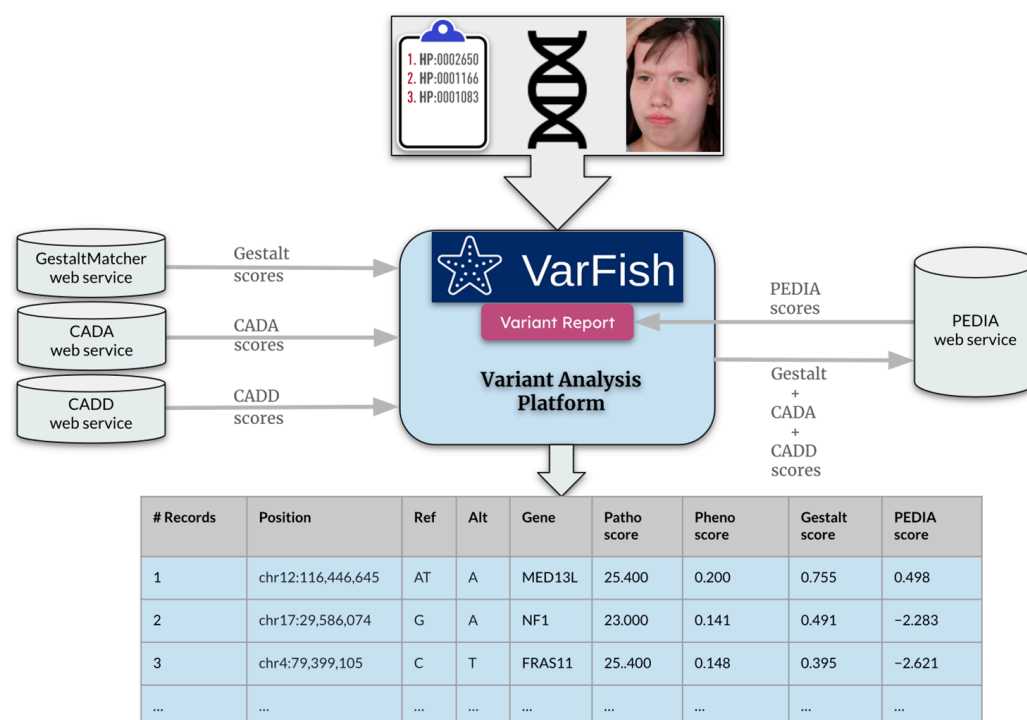


**Figure 1.** Integrating VarFish and PEDIA: Illustration depicting the seamless integration process between VarFish and PEDIA for variant prioritization. Sequencing data in VCF format is imported into VarFish, where filtering is applied. Patient images, not supported by VarFish, are uploaded via a separate web service embedded within VarFish. Gestalt scores per gene are derived using the GestaltMatcher web service. VarFish automatically retrieves CADA scores per gene from the CADA web service and CADD scores for variants from the CADD service. These scores are combined and sent to the PEDIA web service to compute the combined PEDIA score, which is displayed in VarFish’s user interface for variant prioritization. Filtered variants and their scores can be exported as a comprehensive report from VarFish. In this patient, we sorted the variants by PEDIA score in descending order, and the disease-causing mutation in *MED13L* was correctly ranked at the first position. Use of the patient’s image is consented to for publication [31].

## 2. Materials and Methods

### 2.1. Overview

This research focused on a cohort of 163 patients with rare diseases from the TNAMSE project who consented to have their facial images evaluated using GestaltMatcher. VarFish provided a CADD score (molecular level) [32,33], CADA score (feature level) [24], Gestalt-Matcher score (facial level) [25], and PEDIA score [27]. PEDIA combined scores from CADD, CADA, and GestaltMatcher scores using a support vector machine. The step-by-step integration process comprised the following stages: initiating the services individually, configuring VarFish settings, enabling face-based prioritization, and incorporating PEDIA-based prioritization within VarFish. These processes facilitated data transmission among services, aiding in variant filtering and displaying associated scores in a resulting variants table. The evaluation process entailed analyzing data from 163 patients within the cohort by exporting tables from VarFish and identifying the position of the disease-causing gene within sorted PEDIA scores. The performance evaluation included plotting the percentage of cases in which the disease-causing gene appeared within the top 1 to top 100 genes.

### 2.2. Cohort Description

A total of 163 patients diagnosed with rare diseases who provided written informed consent for their facial images to be evaluated using GestaltMatcher and for the results to be utilized in exome variant interpretation were selected from the TNAMSE project. We collected the clinical description encoded in HPO terms, a frontal facial image, and exome sequencing data for each patient. In total, 64 different monogenic disorders were identified. Benchmarking was conducted on the main and validation cohorts from the TNAMSE project. The main cohort comprised 94 patients, with 194 being pediatric cases and 30 adults, representing cases from the actual prospective study of TNAMSE. After the three-year recruitment period, an additional 69 patients were enrolled to form the validation cohort. For simplicity in benchmarking, we combined the main and validation cohorts into a single cohort for analysis in this paper.

### 2.3. Prioritization Approaches

VarFish [30] serves as the analysis platform where sequencing data are uploaded in Variant Call Format (VCF). CADD scores [32] are utilized to predict the deleteriousness of variants, with the input for the CADD service consisting of chromosome number, position, reference, and alternate allele (e.g., 1-25893242-TG-CA). Moreover, VarFish offers a user-friendly graphical interface (GUI) for inputting HPO terms. Furthermore, CADA scores [27] predict pathogenicity by leveraging phenotypic information, with HPO terms serving as inputs for the CADA service. Gestalt scores predict syndromic similarity, with the input for the GestaltMatcher service being the frontal photo of the patient. Ultimately, PEDIA combines these scores to produce a single combined score per gene, utilizing a support vector machine trained on CADD, CADA, and Gestalt scores.

Integrating multiple prioritization tools presents challenges stemming from variations in algorithms, data formats, and the necessity to harmonize diverse outputs for compatibility across tools. To tackle this issue, we seamlessly integrated GestaltMatcher into VarFish using iFrames. iFrames offers a versatile and streamlined approach for embedding external content into web pages, thereby improving functionality, user experience, and facilitating modularity and reusability.

### 2.4. Step-by-Step Setup

The integration between VarFish and other independent tools such as CADA, Gestalt-Matcher, and PEDIA was executed through the following steps:

1. Initialization of Services: VarFish, CADD, CADA, GestaltMatcher, and PEDIA are initiated as separate web services. For instance, these services can be initialized on the same machine but on different ports. Instructions for starting each service can be found in the Supplementary Materials.

2. Configuration in VarFish: VarFish's settings file is configured to include the URLs for the CADD, CADA, GestaltMatcher, and PEDIA web services. This ensures seamless communication and interaction between VarFish and the aforementioned tools. These tools can be hosted either in the same machine for the on-premise solution or accessible via the web services provided by the inventors.
3. Integration of GestaltMatcher into Prioritization:
  - 3.1. The user activates GestaltMatcher within VarFish. The face sender module from the PEDIA middleware is embedded as an iFrame in the prioritization page of VarFish.
  - 3.2. Upon selecting the frontal image of the patient for the case and submitting it, the image is transmitted via the POST method exposed by the REST API endpoint of the GestaltMatcher web service.
  - 3.3. After receiving a successful response from GestaltMatcher, the suggested gene list along with scores is relayed to the parent window of VarFish.
  - 3.4. Additionally, the file name of the last photo successfully submitted to GestaltMatcher is transmitted back to VarFish. This communication from the embedded child frame to the parent window is facilitated using the window.postMessage method.
  - 3.5. A listener is incorporated into the prioritization page of VarFish to capture message events sent from the iFrame. The received data are then stored in the variant query store of VarFish. This process ensures that the patient image does not require re-uploading when the case is reopened in VarFish, as it only needs to be submitted once per case.
  - 3.6. Subsequently, when the user performs filtering, the resulting variants table displays the Gestalt scores obtained from the last image submitted to GestaltMatcher.
4. Enabling PEDIA-based prioritization: within the prioritization page of VarFish, it automatically triggers phenotype-based prioritization using the CADA algorithm. Furthermore, it activates variant pathogenicity-based prioritization utilizing CADD scores, which predict the deleteriousness of the variants.

### 2.5. Automation

To streamline the analysis steps with a huge number of patients and be able to reproduce the results efficiently, we employed the Automa tool (<https://www.automa.site/>, accessed on 20 November 2023), seamlessly integrated as a browser extension. Automa, a specialized automation tool crafted for the efficient execution of repetitive tasks in web browsers, empowers users to construct scripts or workflows. These scripts facilitate programmatic interactions with web browsers, automating tasks seamlessly. In our study, Automa played a pivotal role in automating a series of tasks, including opening a case, configuring diverse filtering criteria, uploading patient photos, enabling prioritization, applying specific filters, and exporting the resulting table comprising variants and scores. The detailed workflow for these tasks using Automa is accessible at (<https://github.com/igsb/pedia-middleware/blob/master/workflow.automa.json>, accessed on 4 February 2024).

## 3. Results

### 3.1. Step-by-Step Analysis

1. The user uploads a case or opens an existing case within VarFish. Within the filtering variants page, the user can customize filter settings according to preferences, such as a population frequency threshold of 1% (Figure 2), specific quality criteria (Figure 3), and variant impact (Figure 4).

	Homozygous-i-plasmy count	Heterozygous-i-plasmy count	Hemizygous count	Frequency / Carriers
<input checked="" type="checkbox"/> 1000 Genomes (samples: 1000)	0	4	Maximal hemi. count in 1000 genomes	0.01
<input checked="" type="checkbox"/> ExAC (samples: 60,706)	0	10	Maximal hemi. count in ExAC	0.01
<input checked="" type="checkbox"/> gnomAD exomes (samples: 125,748)	0	20	Maximal hemi. count in gnomAD exomes	0.01
<input checked="" type="checkbox"/> gnomAD genomes (samples: 15,708)	0	4	Maximal hemi. count in gnomAD genomes	0.01
<input checked="" type="checkbox"/> in-house DB	Maximal in-house hom. count	Maximal in-house het. count	Maximal in-house hemi. count	20
<input checked="" type="checkbox"/> mtDB (samples: ~2704)	10	N/A	N/A	0.01
<input checked="" type="checkbox"/> HelixMTdb (samples: 196,554)	200	Maximal het. count in HelixMTdb	N/A	0.01
<input type="checkbox"/> MITOMAP (samples: 50,174)	Maximal count in MITOMAP	N/A	N/A	Maximal frequency in MITOMAP

**Figure 2.** Frequency filter settings in VarFish. Every row is a different dataset. The user can set the allele frequency filter on the public and in-house datasets.

#	Family	Individual	Father	Mother	min DP het.	min DP hom.	min AB	min GQ	min AD	max AD	on FAIL
1	F_HGACEDIA_040	HGACEDIA_040	0	0	10	5	0.2	10	3		drop variant

**Figure 3.** Quality filter settings in VarFish.

**Variant Types**  
 SNV  indel  MNV

**Transcript Type**  
 coding  non-coding

**Distance to next Exon**  
 max. distance to next exon [input field] bp

**Effect Groups**  
 all  nonsynonymous  splicing  coding  UTR / intronic  non-coding  nonsense

**Detailed Effects**

**Coding**  
 disruptive in-frame deletion  
 disruptive in-frame insertion  feature truncation  
 frameshift elongation  frameshift truncation  
 frameshift variant  inframe deletion  
 inframe insertion  internal elongation  missense  
 MNV  start lost  stop gained  stop retained  
 stop lost  synonymous  tandem duplication

**Off-Exome**  
 downstream  intronic (coding transcript)  
 intergenic  upstream  exon loss

**Non-Coding**  
 3' UTR exonic  3' UTR intronic  5' UTR exonic  
 5' UTR intronic  n.c. exonic  n.c. intronic

**Splicing**  
 splice acceptor  splice donor  splice region

**Structural**  
 structural  transcript ablation

**Extra Annotations**  
 complex substitution

**Figure 4.** Variants and Effects filter settings in VarFish.

- CADA scores are acquired from the CADA web service by transmitting clinical features in HPO terms.
- Subsequently, CADD scores are obtained from the CADD web service by forwarding the filtered variants. The highest CADD score is chosen for each gene.
- Upload the patient's facial image to obtain Gestalt scores calculated by GestaltMatcher (Figure 5).
- After checking the "Enable PEDIA-based prioritization" button and clicking "Filter & Display," these scores (CADA, CADD, and Gestalt) are then dispatched to the PEDIA web service via the REST API endpoint to procure PEDIA scores per gene.
- In the resulting variants table (Figure 6), PEDIA scores are displayed in a distinct column alongside CADA, CADD, and Gestalt scores. Variants associated with genes having higher PEDIA scores are prioritized accordingly.

The screenshot shows the VarFish interface with several settings panels:

- Phenotypic Prioritization:**
  - Enable phenotype-based prioritization (checked).
  - Phenotype Similarity Algorithm: CADA.
  - HPO Terms: HP:0000020 - Urinary incontinence; HP:0000708 - Behavioral abnormality; HP:0000729 - Autistic behavior; HP:0001249 - Intellectual disability; HP:0002607 - Bowel incontinence; HP:0010841 - Multifocal epileptiform discharges.
- Pathogenicity Prioritization:**
  - Enable the pathogenicity-based prioritization and (optionally) adjust the scoring method below.
  - Enable variant pathogenicity-based prioritization (checked).
  - Pathogenicity Score: CADD.
- Face Prioritization:**
  - Enable the GestaltMatcher-based prioritization.
  - Enable GestaltMatcher-based prioritization (checked).
  - Last submitted image to GestaltMatcher: "HGACPEDIA\_040.jpg".
  - Buttons: Choose File (HGACPEDIA\_040.jpg), Submit to GestaltMatcher.
- Combined Prioritization:**
  - Enable PEDIA based prioritization (checked).
  - Notes: PEDIA is "Prioritization of Exome Data by Image Analysis". It combines phenotypic, pathogenic and facial scores together to produce a single score per gene. Selecting PEDIA based prioritization will automatically enable all of the following prioritization configurations:
    - 1. Phenotype based prioritization with "CADA" algorithm.
    - 2. Variant pathogenicity-based prioritization with "CADD" scores.
    - 3. GestaltMatcher-based prioritization.

**Figure 5.** Enabling the PEDIA-based prioritization requires the following settings: phenotypic prioritization using the CADA algorithm, variant pathogenicity-based prioritization using CADD, and face-based prioritization with images successfully submitted to GestaltMatcher.

#	variant icons	position	ref	alt	frequency	#hom	constraint	gene	gene icons	Effect	HGACPEDIA_040	patho score	pheno score	patho+pheno score	Gestalt score	PEDIA score
1		chr12:118,446,645	AT	A	0.00000	0	1.000	MED13L		p.K524Nfs*17	0/1	25.400	0.200	5.080	0.755	0.498
2		chr17:29,586,074	G	A	0.00002	0	0.902	NF1		p.V1432I	0/1	23.000	0.141	3.243	0.491	-2.283
3		chr4:78,389,105	C	T	0.00002	0	0.000	FRAS1		p.A2663V	0/1	25.400	0.140	3.748	0.395	-2.621
4		chr2:74,072,313	T	A	0.00001	0	0.000	STAMBP		p.F100Y	0/1	28.900	0.137	3.955	0.304	-3.119
5		chr4:73,101,425	T	C	0.00007	0	0.000	ADAMTS3		p.R390R	0/1	24.800	0.143	3.510	0.291	-3.418
6		chr20:45,353,746	A	T	0.00000	0	0.000	SLC2A10		p.Y24F	0/1	24.900	0.105	2.612	0.339	-3.683
7		chr4:15,542,462	C	T	0.00000	0	0.000	CC2D2A		p.A669V	0/1	0.787	0.173	0.136	0.402	-3.939
8		chr11:45,957,292	TAAA...	T	0.00000	0	1.000	PIHF21A		c.1682-0_168...	0/1	9.361	0.151	1.412	0.337	-4.086
9		chr2:170,042,416	G	T	0.00003	0	1.000	LRP2		c.9442C>A	0/1	7.528	0.149	1.119	0.343	-4.213
10		chrX:128,170,361	A	G	0.00001	0	1.000	OCRL		c.1947A>G	0/1	9.320	0.130	1.213	0.353	-4.311
11		chr4:81,124,209	C	G	0.00000	0	0.776	PRDM8		c.1583C>G	0/1	12.330	0.252	3.104	0.000	-4.440
12		chr4:6,303,072	G	A	0.00004	0	0.000	WFS1		p.R517H	0/1	27.200	0.177	4.821	0.000	-4.546
13		chr5:10,380,488	C	T	0.00004	0	1.000	MARCHF6		p.T103M	0/1	24.200	0.181	4.374	0.000	-4.706
14		chr2:96,963,274	C	T	0.00000	0	1.000	SNRNP200		p.A402T	0/1	23.000	0.186	4.281	0.000	-4.707
15		chr11:76,858,959	G	A	0.00003	0	0.000	MYO7A		p.R33H	0/1	25.900	0.172	4.449	0.000	-4.721
16		chr17:73,231,736	C	T	0.00003	0	1.000	NUPR5		p.R645W	0/1	24.800	0.163	4.031	0.000	-4.949
17		chr11:67,379,370	G	A	0.00001	0	0.000	NDUFP1		c.1056G>A	0/1	8.006	0.229	1.633	0.000	-5.107
18		chr8:133,141,740	G	A	0.00000	0	0.801	KCNQ3		c.2028C>T	0/1	10.330	0.218	2.250	0.000	-5.116
19		chr2:98,853,101	C	A	0.00000	0	0.000	VWA3B		p.L861I	0/1	12.040	0.208	2.508	0.000	-5.143

**Figure 6.** The results table of VarFish shows the variants sorted/ranked by the PEDIA scores after the filtering is performed. The CADA, CADD, and Gestalt scores are also shown in the table to increase the explainability of how the final PEDIA score was obtained. The disease-causing mutation in *MED13L* was correctly ranked at the first position.

### 3.2. Visualizing Results in VarFish

The user can sort the variants based on the different scores (Figure 6), allowing for prioritization of the candidate list. Additionally, they can export the resulting table as an Excel or TSV (Tab-Separated Values) file for further analysis and documentation. This functionality provides flexibility and convenience in managing and presenting the variant data. For example, the patient presenting in Figures 6 and 7 was molecularly diagnosed with Impaired Intellectual Development and Distinctive Facial Features with or without Cardiac Defects (OMIM: 616789). When we sorted the variants by PEDIA scores, the disease-causing mutation in *MED13L* was correctly ranked in the top position (Figure 6). Moreover, visualizing the distribution of PEDIA scores by Manhattan plot (Figure 7), we can see that the PEDIA score of *MED13L* is higher than zero and clearly on top of the other genes.

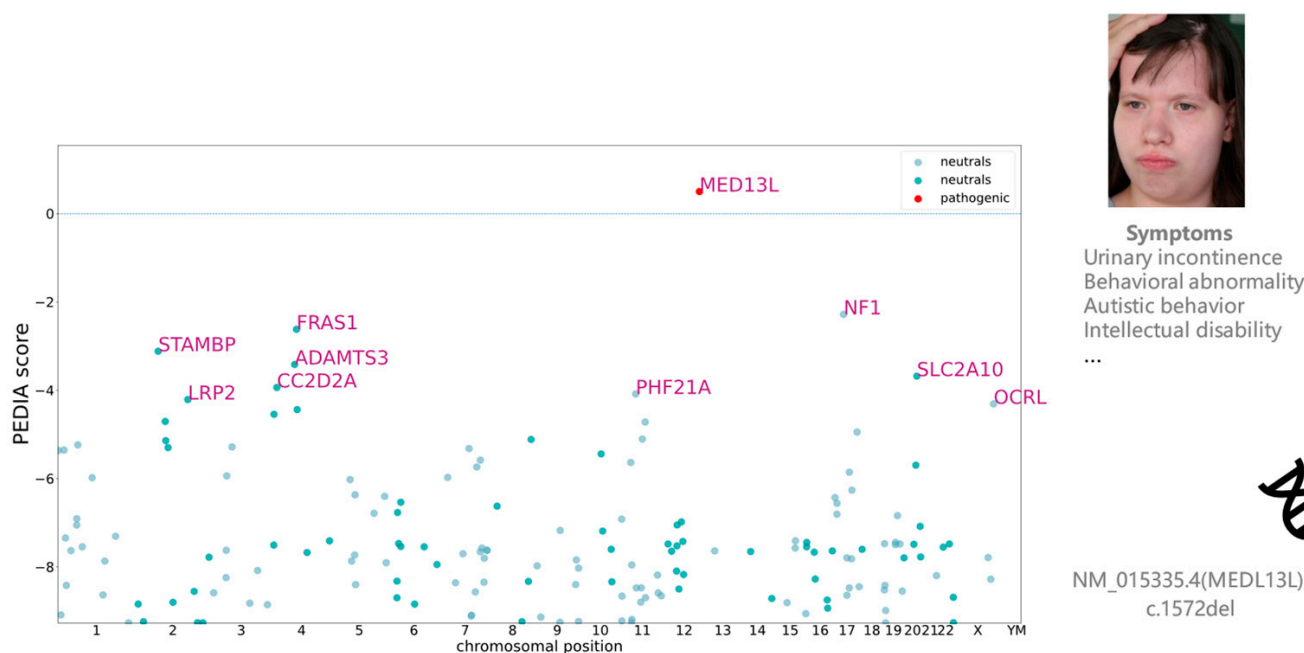


**Figure 7.** This is an illustrative case where the disease-causing gene achieves the highest PEDIA score, confirming the diagnosis of Impaired Intellectual Development and Distinctive Facial Features with or without Cardiac Defects (OMIM: 616789). *MED13L* was ranked first in this case, providing molecular confirmation of the diagnosis.

### 3.3. Performance Comparison

We analyzed the 163 cases in the TNAMSE study. We plotted the percentage of cases concerning the top-ranking genes to visualize the performance (Figure 8). Our study encompassed the assessment of top-1, top-10, and top-100 accuracy within both primary and validation cohorts. We compared the performance of using CADD, CADA, GestaltMatcher solely, CADA plus CADD, and PEDIA. Figure 8 shows that with the PEDIA score, the disease-causing gene of 57.67% of patients was ranked in the top one position, and 83.44% were ranked in the top ten. In top ten accuracy, PEDIA is 7.37% higher than using CADD plus CADA (molecular and feature scores), and the PEDIA approach outperformed all the other score settings.

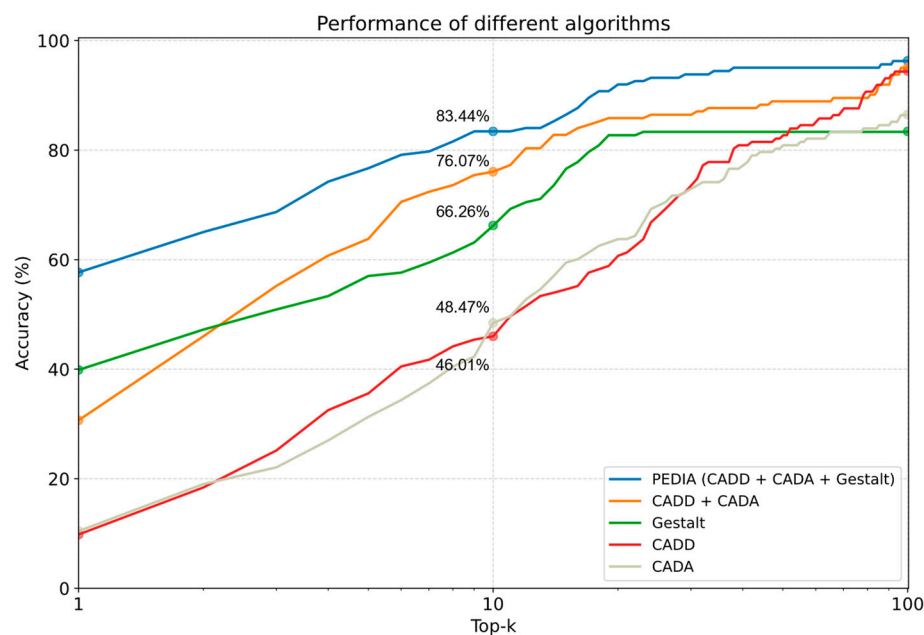


**Figure 8.** Specifically, on the y-axis, we represented the percentage of cases wherein the disease-causing gene appeared at positions ranging from top 1 to top 100. The x-axis denoted the top k genes. The Gestalt score utilizes facial image analysis through GestaltMatcher. The CADD score is derived from molecular pathogenicity assessments. CADA relies on clinical feature analysis. PEDIA integrates these three scores for variant prioritization.

#### 4. Discussion

This study showcases the integration of GestaltMatcher and PEDIA within VarFish, an open-source variant analysis framework. However, the previous version of the PEDIA approach relied on the support of DeepGestalt from the Face2Gene platform run by FDNA Inc. for the gestalt scores. The non-open-source nature of DeepGestalt posed challenges for its integration into any variant prioritization platform. To address this, we replaced DeepGestalt with an open-source version of GestaltMatcher [28] provided by the Institute for Genomic Statistics and Bioinformatics at University Hospital of Bonn, making the models accessible to the research community. Facial images are considered sensitive data, and many patients are reluctant to consent to data transfer outside of the hospital. Therefore, an on-premise solution is essential for such integrations. This initiative enabled GestaltMatcher to function as an on-premise solution, allowing users to analyze patient images without requiring data transfer consent. The successful integration of GestaltMatcher and PEDIA within VarFish serves as an exemplary model for developers seeking on-premise solutions. It demonstrates how facial analysis can seamlessly be integrated into various platforms, facilitating broader adoption and utilization across domains.

In Figures 6 and 7, the disease-causing mutation was ranked at the top one position, despite it having relatively low CADD and CADA scores. Upon examining the entire cohort comprising 163 patients, it was found that the disease-causing gene of 57.67% of patients was ranked at the top one position, while that of 83.44% was ranked within the top ten. These findings underscore the significant performance of PEDIA compared to other scores, indicating its efficacy in facilitating variant prioritization.

This study does not assert that the current PEDIA approach, which combines CADD, CADA, and Gestalt scores, represents the state-of-the-art method for prioritizing exome variants. Rather, the PEDIA study merely demonstrates that integrating facial image analysis with feature and molecular scores can significantly enhance performance. In the future, further benchmarking of various combinations of available tools, such as LIRICAL [11], AMELIE [6], and Exomizer [32,33], could provide additional insights. Moreover, considering that the GestaltMatcher Database adheres to the FAIR (Findable, Accessible, In-

teroperable, and Reusable) principles, we anticipate the emergence of numerous advanced facial analysis approaches in the near future.

Incorporating the PEDIA not only enhances performance, but also minimally impacts runtime and hardware requirements. GestaltMatcher operates efficiently without the need for GPU installation, analyzing an image in approximately seven seconds. With GPU support, this analysis time can be reduced to around three seconds. Additionally, the CADA analysis also completes within a few seconds. However, assessing the overall runtime of VarFish is challenging due to variations in annotation databases and filtering parameters. Typically, filtering exome data for a single patient takes only a few minutes. Notably, VarFish recommends a minimum of 16 CPU cores, 64 GB RAM, and 300 GB storage. As such, any increase in the overall runtime of the PEDIA process is likely negligible. It also indicates that PEDIA can be implemented in any platform.

In the future, it will be crucial for facial analysis to provide additional evidence supporting the ACMG (American College of Medical Genetics and Genomics) variant classification guidelines [34,35]. For instance, integrating features that align with the PP4 criteria, which assesses phenotype match (i.e., whether a patient's phenotype or family history is highly specific for a disease with a single genetic etiology), could be valuable. This kind of evidence would be particularly beneficial in addressing the challenge of Variants of Unknown Significance (VUS) by potentially reclassifying them as likely pathogenic, thus providing more precise clinical guidance.

## 5. Conclusions

In conclusion, this study effectively integrates GestaltMatcher and PEDIA within VarFish, overcoming challenges related to data privacy and closed-source components. PEDIA demonstrates strong performance in prioritizing disease-causing genes, highlighting its potential in variant prioritization. Future advancements in facial analysis supporting ACMG guidelines are essential for improving clinical decision making, particularly regarding VUS.

**Supplementary Materials:** The following supporting information can be downloaded at: <https://www.mdpi.com/article/10.3390/genes15030370/s1>.

**Author Contributions:** Methodology, M.A.B. and A.S.; software, M.A.B., P.I., A.S. and M.H.; writing—original draft preparation, M.A.B. and A.K.; writing—review and editing, T.-C.H.; supervision, T.-C.H. and P.M.K.; clinical supervision, M.E.; project administration, T.-C.H. and A.K. All authors have read and agreed to the published version of the manuscript.

**Funding:** This research received no external funding.

**Institutional Review Board Statement:** Not applicable.

**Informed Consent Statement:** Informed consent was obtained from all subjects involved in the study.

**Data Availability Statement:** The source code for this project is accessible on GitHub at the following URLs: <https://github.com/ahujameg/varfish-server>, accessed on 12 March 2024 and <https://github.com/igsb/pedia-middleware>, accessed on 1 March 2024 (v1.0). The documentation can be found in PEDIA-middleware ReadTheDocs (<https://pedia-middleware.readthedocs.io/en/latest/index.html>, accessed on 29 February 2024). The data supporting this research are available upon request. Please contact Dr. Tzung-Chien Hsieh to request access to the data.

**Acknowledgments:** We acknowledge support from the TRANSLATE-NAMSE project.

**Conflicts of Interest:** The authors declare no conflicts of interest.

## References

1. Ferreira, C.R. The burden of rare diseases. *Am. J. Med. Genet. A* **2019**, *179*, 885–892. [[CrossRef](#)] [[PubMed](#)]
2. Chung, C.C.; Leung, G.K.; Mak, C.C.; Fung, J.L.; Lee, M.; Pei, S.L.; Yu, M.H.; Hui, V.C.; Chan, J.C.; Chau, J.F.; et al. Rapid whole-exome sequencing facilitates precision medicine in paediatric rare disease patients and reduces healthcare costs. *Lancet Reg. Health West. Pac.* **2020**, *1*, 100001. [[CrossRef](#)] [[PubMed](#)]

3. Köhler, S.; Gargano, M.; Matentzoglou, N.; Carmody, L.C.; Lewis-Smith, D.; Vasilevsky, N.A.; Danis, D.; Balagura, S.; Baynam, G.; Brower, A.M.; et al. The Human Phenotype Ontology in 2021. *Nucleic Acids Res.* **2021**, *49*, D1207–D1217. [[CrossRef](#)] [[PubMed](#)]
4. Köhler, S.; Schulz, M.H.; Krawitz, P.; Bauer, S.; Dölken, S.; Ott, C.E.; Mundlos, C.; Horn, D.; Mundlos, S.; Robinson, P.N. Clinical Diagnostics in Human Genetics with Semantic Similarity Searches in Ontologies. *Am. J. Hum. Genet.* **2009**, *85*, 457–464. [[CrossRef](#)] [[PubMed](#)]
5. Bauer, S.; Köhler, S.; Schulz, M.H.; Robinson, P.N. Bayesian ontology querying for accurate and noise-tolerant semantic searches. *Bioinformatics* **2012**, *28*, 2502–2508. [[CrossRef](#)] [[PubMed](#)]
6. Smedley, D.; Jacobsen, J.O.B.; Jäger, M.; Köhler, S.; Holtgrewe, M.; Schubach, M.; Siragusa, E.; Zemojtel, T.; Buske, O.J.; Washington, N.L.; et al. Next-generation diagnostics and disease-gene discovery with the Exomiser. *Nat. Protoc.* **2015**, *10*, 2004–2015. [[CrossRef](#)] [[PubMed](#)]
7. Yang, H.; Robinson, P.N.; Wang, K. Phenolyzer: Phenotype-based prioritization of candidate genes for human diseases. *Nat. Methods* **2015**, *12*, 841–843. [[CrossRef](#)]
8. Jagadeesh, K.A.; Birgmeier, J.; Guturu, H.; Deisseroth, C.A.; Wenger, A.M.; Bernstein, J.A.; Bejerano, G. Phrank measures phenotype sets similarity to greatly improve Mendelian diagnostic disease prioritization. *Genet. Med.* **2019**, *21*, 464–470. [[CrossRef](#)]
9. Birgmeier, J.; Haeussler, M.; Deisseroth, C.A.; Steinberg, E.H.; Jagadeesh, K.A.; Ratner, A.J.; Guturu, H.; Wenger, A.M.; Diekhans, M.E.; Stenson, P.D.; et al. AMELIE speeds Mendelian diagnosis by matching patient phenotype and genotype to primary literature. *Sci. Transl. Med.* **2020**, *12*, eaau9113. [[CrossRef](#)]
10. Zhao, M.; Havrilla, J.M.; Fang, L.; Chen, Y.; Peng, J.; Liu, C.; Wu, C.; Sarmady, M.; Botas, P.; Isla, J.; et al. Phen2Gene: Rapid phenotype-driven gene prioritization for rare diseases. *NAR Genom. Bioinform.* **2020**, *2*, lqaa032. [[CrossRef](#)]
11. Robinson, P.N.; Ravanmehr, V.; Jacobsen, J.O.; Danis, D.; Zhang, X.A.; Carmody, L.C.; Gargano, M.A.; Thaxton, C.L.; Karlebach, G.; Reese, J.; et al. Interpretable Clinical Genomics with a Likelihood Ratio Paradigm. *Am. J. Hum. Genet.* **2020**, *107*, 403–417. [[CrossRef](#)]
12. Peng, C.; Dieck, S.; Schmid, A.; Ahmad, A.; Knaus, A.; Wenzel, M.; Mehnert, L.; Zirn, B.; Haack, T.; Ossowski, S.; et al. CADA: Phenotype-driven gene prioritization based on a case-enriched knowledge graph. *NAR Genom. Bioinform.* **2021**, *3*, lqab078. [[CrossRef](#)]
13. Chen, Z.; Zheng, Y.; Yang, Y.; Huang, Y.; Zhao, S.; Zhao, H.; Yu, C.; Dong, X.; Zhang, Y.; Wang, L.; et al. PhenoApt leverages clinical expertise to prioritize candidate genes via machine learning. *Am. J. Hum. Genet.* **2022**, *109*, 270–281. [[CrossRef](#)]
14. Kelly, C.; Szabo, A.; Pontikos, N.; Arno, G.; Robinson, P.N.; Jacobsen, J.O.; Smedley, D.; Cipriani, V. Phenotype-aware prioritisation of rare Mendelian disease variants. *Trends Genet.* **2022**, *38*, 1271–1283. [[CrossRef](#)]
15. Zhai, W.; Huang, X.; Shen, N.; Zhu, S. Phen2Disease: A phenotype-driven model for disease and gene prioritization by bidirectional maximum matching semantic similarities. *Brief. Bioinform.* **2023**, *24*, bbad172. [[CrossRef](#)] [[PubMed](#)]
16. Yang, J.; Liu, C.; Deng, W.; Wu, D.; Weng, C.; Zhou, Y.; Wang, K. Enhancing phenotype recognition in clinical notes using large language models: PhenoBCBERT and PhenoGPT. *Patterns* **2024**, *5*, 100887. [[CrossRef](#)] [[PubMed](#)]
17. Dudding-Byth, T.; Baxter, A.; Holliday, E.G.; Hackett, A.; O'donnell, S.; White, S.M.; Attia, J.; Brunner, H.; De Vries, B.; Koolen, D.; et al. Computer face-matching technology using two-dimensional photographs accurately matches the facial gestalt of unrelated individuals with the same syndromic form of intellectual disability. *BMC Biotechnol.* **2017**, *17*, 90. [[CrossRef](#)] [[PubMed](#)]
18. Shukla, P.; Gupta, T.; Saini, A.; Singh, P.; Balasubramanian, R. A Deep Learning Frame-Work for Recognizing Developmental Disorders. In Proceedings of the 2017 IEEE Winter Conference on Applications of Computer Vision (WACV), Santa Rosa, CA, USA, 24–31 March 2017; pp. 705–714.
19. Liehr, T.; Acquarola, N.; Pyle, K.; St-Pierre, S.; Rinholm, M.; Bar, O.; Wilhelm, K.; Schreyer, I. Next generation phenotyping in Emanuel and Pallister-Killian syndrome using computer-aided facial dysmorphology analysis of 2D photos. *Clin. Genet.* **2018**, *93*, 378–381. [[CrossRef](#)] [[PubMed](#)]
20. van der Donk, R.; Jansen, S.; Schuurs-Hoeijmakers, J.H.M.; Koolen, D.A.; Goltstein, L.C.M.J.; Hoischen, A.; Brunner, H.G.; Kemmeren, P.; Nellåker, C.; Vissers, L.E.L.M.; et al. Next-generation phenotyping using computer vision algorithms in rare genomic neurodevelopmental disorders. *Genet. Med.* **2019**, *21*, 1719–1725. [[CrossRef](#)]
21. Gurovich, Y.; Hanani, Y.; Bar, O.; Nadav, G.; Fleischer, N.; Gelbman, D.; Basel-Salmon, L.; Krawitz, P.M.; Kamphausen, S.B.; Zenker, M.; et al. Identifying facial phenotypes of genetic disorders using deep learning. *Nat. Med.* **2019**, *25*, 60–64. [[CrossRef](#)]
22. Liu, H.; Mo, Z.-H.; Yang, H.; Zhang, Z.-F.; Hong, D.; Wen, L.; Lin, M.-Y.; Zheng, Y.-Y.; Zhang, Z.-W.; Xu, X.-W.; et al. Automatic Facial Recognition of Williams-Beuren Syndrome Based on Deep Convolutional Neural Networks. *Front. Pediatr.* **2021**, *9*, 648255. [[CrossRef](#)]
23. Porras, A.R.; Rosenbaum, K.; Tor-Diez, C.; Summar, M.; Linguraru, M.G. Development and evaluation of a machine learning-based point-of-care screening tool for genetic syndromes in children: A multinational retrospective study. *Lancet Digit. Health* **2021**, *3*, e635–e643. [[CrossRef](#)] [[PubMed](#)]
24. Hong, D.; Zheng, Y.-Y.; Xin, Y.; Sun, L.; Yang, H.; Lin, M.-Y.; Liu, C.; Li, B.-N.; Zhang, Z.-W.; Zhuang, J.; et al. Genetic syndromes screening by facial recognition technology: VGG-16 screening model construction and evaluation. *Orphanet J. Rare Dis.* **2021**, *16*, 344. [[CrossRef](#)] [[PubMed](#)]

25. Hsieh, T.-C.; Bar-Haim, A.; Moosa, S.; Ehmke, N.; Gripp, K.W.; Pantel, J.T.; Danyel, M.; Mensah, M.A.; Horn, D.; Rosnev, S.; et al. GestaltMatcher facilitates rare disease matching using facial phenotype descriptors. *Nat. Genet.* **2022**, *54*, 349–357. [[CrossRef](#)] [[PubMed](#)]
26. Schmidt, A.; Danyel, M.; Grundmann, K.; Brunet, T.; Klinkhammer, H.; Hsieh, T.-C.; Engels, H.; Peters, S.; Knaus, A.; Moosa, S.; et al. Next-generation phenotyping integrated in a national framework for patients with ultra-rare disorders improves genetic diagnostics and yields new molecular findings. *medRxiv* **2023**. [[CrossRef](#)]
27. Hsieh, T.-C.; Mensah, M.A.; Pantel, J.T.; Aguilar, D.; Bar, O.; Bayat, A.; Becerra-Solano, L.; Bentzen, H.B.; Biskup, S.; Borisov, O.; et al. PEDIA: Prioritization of exome data by image analysis. *Genet. Med.* **2019**, *21*, 2807–2814. [[CrossRef](#)] [[PubMed](#)]
28. Hsieh, T.-C.; Lesmann, H.; Krawitz, P.M. Facilitating the Molecular Diagnosis of Rare Genetic Disorders Through Facial Phenotypic Scores. *Curr. Protoc.* **2023**, *3*, e906. [[CrossRef](#)] [[PubMed](#)]
29. Lesmann, H.; Lyon, G.J.; Caro, P.; Abdelrazek, I.M.; Moosa, S.; Pantel, J.T.; Klinkhammer, H.; Hagen, M.T.; Kamphans, T.; Meiswinkel, W.; et al. GestaltMatcher Database—A FAIR database for medical imaging data of rare disorders. *medRxiv* **2023**. [[CrossRef](#)]
30. Holtgrewe, M.; Stolpe, O.; Nieminen, M.; Mundlos, S.; Knaus, A.; Kornak, U.; Seelow, D.; Segebrecht, L.; Spielmann, M.; Fischer-Zirnsak, B.; et al. VarFish: Comprehensive DNA variant analysis for diagnostics and research. *Nucleic Acids Res.* **2020**, *48*, W162–W169. [[CrossRef](#)]
31. Elbracht, M. GestaltMatcher Database Case. 7274. Available online: <https://db.gestaltmatcher.org/id/7274> (accessed on 2 February 2024).
32. Kircher, M.; Witten, D.M.; Jain, P.; O’Roak, B.J.; Cooper, G.M.; Shendure, J. A general framework for estimating the relative pathogenicity of human genetic variants. *Nat. Genet.* **2014**, *46*, 310–315. [[CrossRef](#)]
33. Rentzsch, P.; Witten, D.; Cooper, G.M.; Shendure, J.; Kircher, M. CADD: Predicting the deleteriousness of variants throughout the human genome. *Nucleic Acids Res.* **2019**, *47*, D886–D894. [[CrossRef](#)] [[PubMed](#)]
34. Richards, S.; Aziz, N.; Bale, S.; Bick, D.; Das, S.; Gastier-Foster, J.; Grody, W.W.; Hegde, M.; Lyon, E.; Spector, E.; et al. Standards and guidelines for the interpretation of sequence variants: A joint consensus recommendation of the American College of Medical Genetics and Genomics and the Association for Molecular Pathology. *Genet. Med.* **2015**, *17*, 405–424. [[CrossRef](#)] [[PubMed](#)]
35. Tavtigian, S.V.; Greenblatt, M.S.; Harrison, S.M.; Nussbaum, R.L.; Prabhu, S.A.; Boucher, K.M.; Biesecker, L.G. Modeling the ACMG/AMP variant classification guidelines as a Bayesian classification framework. *Genet. Med.* **2018**, *20*, 1054–1060. [[CrossRef](#)] [[PubMed](#)]

**Disclaimer/Publisher’s Note:** The statements, opinions and data contained in all publications are solely those of the individual author(s) and contributor(s) and not of MDPI and/or the editor(s). MDPI and/or the editor(s) disclaim responsibility for any injury to people or property resulting from any ideas, methods, instructions or products referred to in the content.